THE UNIVERSITY OF MICHIGAN
INDUSTRY PROGRAM OF THE COLLEGE OF ENGINEERING

EVALUATION OF A VARIABLE MACH NUMBER SLIDING BLOCK NOZZLE IN THE MACH NUMBER RANGE 1.3 TO 4.0

James L. Amick
Hans Peter Liepman
Theodore H. Reynolds

June, 1957

IP-221

TABLE OF CONTENTS

LIST OF FIGURES

ABSTRACT

A sliding block wind tunnel nozzle was developed and tested at Mach numbers from 1.3 to 4.0 in the Supersonic Wind Tunnel Facility of the University of Michigan's Department of Aeronautical Engineering. In this range the Mach number deviation from the average within a test rhombus is less than $\pm$ 0.9% and the flow angle deviation less than $\pm$ 0.5°. The throat-to-test rhombus distance at the highest Mach number is 8.8 times the test-rhombus height. Overall pressure ratios required are about the same as those of conventional wind tunnels.

I. INTRODUCTION

Variable Mach number nozzles have many potential advantages over the fixed-block type of nozzle for producing supersonic flow in wind tunnels. One promising type of variable nozzle, the asymmetric sliding-block type, has been shown to give good performance at Mach numbers below 3.0 (References 1-3). In order to extend the Mach number range of such a nozzle, the present investigation was begun early in 1951 under Air Force sponsorship.* The objective was to determine contours of a sliding-block nozzle for the range M = 1.4 to 4.0, with experimental verification of satisfactory flow uniformity throughout the range.

The theoretical contours of the experimental nozzle were derived from the method of characteristics (Reference 4). The mechanical design of the nozzle consisted of a flexible plate-jack system for each contour which could also be rotated as a unit about a pivot near the throat (Reference 6). This made it possible to make experimental corrections to the theoretical contours to achieve the most uniform flow in the test section over the widest range of Mach numbers possible.

This paper presents the major results of the experimental work, the details of which can be found in Reference 7.

---

* This work was sponsored by the Aeronautical Research Laboratory, Air Research and Development Command, U.S. Air Force, under Contract 33(038)23070.

II. EXPERIMENTAL APPARATUS

Description of Nozzle

A 4- by 4-inch model of the nozzle (Reference 6) was built in order to evaluate the theoretical contours and to make experimental corrections, if necessary. The nozzle was connected to the existing dry-air storage tank by entrance ducting and screens, and to the existing vacuum tank by an adjustable supersonic diffuser, fixed subsonic diffuser, and valves. The nozzle blocks consisted of flexible plates supported by jacks, with inflexible portions in the test section and subsonic region. In addition to the jack motion, each nozzle block could be rotated as a whole about a point near the throat. The sliding of the lower block to control Mach number was always in a direction parallel to the theoretical test-section axis, even with the block rotated. Plate glass windows measuring 8 by 41 inches extended from near the throat to about 4 inches downstream of the nozzle exit. Inflatable seals in grooves along the nozzle-block edges sealed the joints between the blocks and the windows or sideplates. An overall view of the tunnel with one side removed is shown in Fig. 1.

Pitot Rake

Pitot pressures were measured with a five-prong rake. The prongs on the rake are 1-1/4 inches long and are spaced 1/2 inch apart. They are constructed of 17-gage (.058 OD, .042 ID) type-304 stainless steel hypodermic tubing, with the open end beveled 10° to a sharp inside edge. The body of the rake has a 2-1/4-inch span, 1/4-inch thickness,

and 1-1/4-inch chord, with a sharp 45° edge at both leading and trailing edges, and it attaches to a 10-inch sting which can be moved axially from outside the tunnel. Vertical position and angle of attack can also be changed during a run. Mercury manometers were used in conjunction with the pitot rake during both atmospheric and higher stagnation pressure runs.

A similar three-prong rake was used for some of the low Mach number work where the five-prong rake caused local blocking. A single pitot probe was also available.

Flow Inclinometer

Flow inclination was measured with a wedge-type flow inclinometer. The flow inclinometer has five pairs of 0.042-inch diameter orifices spaced at 0.380-inch intervals spanwise, 0.350 inches from the leading edge. The plan form is rectangular, with a 2-inch span, 1/2-inch thickness, and 1-1/2-inch chord, and the wedge angle is 45° at both the leading and trailing edges. The flow inclinometer attaches to the probe support, thus enabling it to be moved axially, vertically, and to an angle of attack. The pressure difference between the orifices of each pair were measured by manometers using Meriam red oil of specific gravity 0.827. The sensitivity of these pressure differences to flow inclination was calibrated for each Mach number.

A second flow inclinometer, having a wedge angle of 12°, was available for use at low Mach numbers.

Static Orifices

There are 24 1/32-inch-diameter static orifices along the lower nozzle contour, and 12 along the upper. Twenty of the lower-contour orifices lie along the straight portion of the block at 1-inch intervals. These static orifices were connected to manometer tubes filled with Meriam red oil. Only relative pressures were measured, because of the inconvenience of measuring absolute pressures with such a light fluid.

Static needle rakes were available but were not used because of the shock-free nature of the flow. It was reasoned that, in the absence of shocks, the flow through the nozzle should be essentially isentropic and, therefore, Mach numbers in the test section could be calculated from pitot and reservoir pressure measurements alone.

Schlieren System

An 8-inch schlieren system was used for the qualitative analysis of the flow. This system proved to be useful for observation of starting and stopping shocks and boundary layer-probe shock interaction. However, the weak shock waves usually seen in schlieren pictures of supersonic flow were either absent or so weak as to be hidden by the mottled background produced by the commercial-quality surface finish on the plate glass windows.

III. DEVELOPMENT OF NOZZLE CONTOURS

Theoretical Contours

The nozzle contour design, given in detail in Reference 4, followed the iterative characteristic method outlined by Burbank and Byrne in Reference 3, with helpful suggestions by Dr. A. Ferri. Design Mach numbers of 1.64 and 3.87 were employed, and a throat test-section axis-inclination angle of 16° was used. Characteristic nets for intermediate Mach numbers of 2.37, 3.23, and 4.01 were also constructed. The following criteria were established to guide the construction of the characteristic nets:

(1) The sonic line was to be straight and perpendicular to the nozzle contour.

(2) No inflection points were to be used in the supersonic controus.

(3) The first derivative of the contours was to be smooth and continuous.

Values of the second derivative along the contours were obtained by fairing and differentiating the slopes given by the characteristic nets. The second derivatives were then faired and integrated twice to obtain the contour coordinates. The subsonic portions were designed by one-dimensional theory, observing the requirement that the throat curvature should be essentially zero for 1 to 1-1/2 throat-heights upstream of the sonic line, in order to insure a straight, perpendicular sonic line.

Tests and Results with Theoretical Contours

For the first tests in the evaluation of the nozzle, the jacks were positioned so that the contours of each block by itself duplicated the theoretical inviscid contours. The flow produced by the nozzle was evaluated with the pitot rake, flow inclinometer, and static orifices. These measurements showed that the difference of extreme Mach numbers in a test rhombus 3.6 inches high varied between 1.6% at M = 1.5 and 3.8% at M = 3.2 The maximum difference in flow angle varied between 0.7° and 2.2° at the same Mach numbers. The major nonuniformity at all Mach numbers above 2.5 was a band of compression waves of about $1\text{-}1/2^{\circ}$ total deflection angle, originating in (or reflecting from) the vicinity of the last three jacks on the upper contour.

No shock waves were detected in either the schlieren observations or the moving-probe tests. This absence of shock waves is attributed to the lack of physical junctures in the supersonic portion of the nozzle, and the lack of contour waviness of short wavelength.

In choosing the value 3.6 inches for the test rhombus height, it was assumed that Mach waves impinging on the boundary layer would curve as they entered the boundary layer, become normal to the wall, and reflect back along another curve to the outer edge of the boundary layer. As far as the reflected Mach wave is concerned, the process could be considered one of specular reflection from a "reflection" plane parallel to the wall within the boundary layer. In this and the following flow evaluations it was arbitrarily assumed

that the reflection thickness (distance of this reflection surface from the wall) was 0.2 inches at all Mach numbers. This value represents about one-half to one-quarter of the boundary layer thickness, depending on the Mach number. The effective test rhombus height is then the actual height minus twice the reflection thickness.

Improvement of Flow Uniformity

Rotation. The first change in nozzle configuration made to improve the flow uniformity consisted of an outward rotation of the downstream ends of both nozzle blocks, to effect a linear boundary layer correction. The changes in flow uniformity produced by this correction were small.

Sidewall Fences. It was suspected that the flow non-uniformity might be caused at least partly by excessive thickening of the floor boundary layer due to downward flow in the sidewall boundary layers. This was confirmed in tests utilizing the china clay method of visualization of boundary layer streamlines. Aluminum fences were then glued to the glass sidewalls, following the recommendations of Reference 8. Combinations of 3, 5, and 7 fences on each sidewall were tested at $M = 3.0$. In each case the flow uniformity, as measured with the flow inclinometer, showed no improvement. There appeared, however, to be some reduction in boundary-layer cross flow on the sides as shown by china clay streamlines.

Boundary Layer Corrections. Several different boundary layer corrections were set into the contours by adjustment of the jacks. The first correction consisted of an outward movement of the

contour at each station by an amount equal to the displacement thickness on the contour at that station. The displacement thicknesses were calculated by the Tucker method (Reference 9) for flow at M = 3.2, assuming zero boundary-layer thickness at the throat. The boundary layer thickness at the nozzle exit, calculated by this method, was in reasonable agreement with that obtained from pitot probe measurements of actual boundary layer. The variation of boundary-layer displacement thickness in the test section was taken to be a straight line extension of that at the exit of the nozzle.

The flow produced by the nozzle with this boundary-layer correction was measured with the pitot rake connected to mercury manometers. A definite improvement in flow uniformity was noted. The maximum Mach number variation within a 4-inch-high test rhombus was reduced to 2.6 percent or less over the whole Mach number range.

Next, nozzle blocks were rotated outward to make a linear correction for the sidewall boundary-layer displacement thickness in addition to that of the contoured walls. Due to mechanical limitations, however, only 0.9 of the sidewall displacement thickness at M = 3.2 could be corrected for. Tests with this nozzle setting showed only a slight improvement in uniformity over that of the two-wall correction. Due to the increased test-section height, a Mach number of 4.1 was reached with the lower block translated to its upstream limit; with the two-wall correction, the corresponding upper limit was a Mach number of 3.9.

Final Correction. The final contour setting was arrived at by going back to the two-wall displacement-thickness correction with test-section boundary-layer growth extrapolated linerly from that at the nozzle exit. This contour was accurately set by means of the height gage and straight edge. Some small changes were then made in the downstream part of the upper contour, which improved the flow slightly at the higher Mach numbers, where the greatest nonuniformities had existed in the flow with the unmodified boundary-layer correction. The flow produced by these final contours was then evaluated in great detail by means of pitot probe and static-wall pressure tests. The results of these tests, presented below, show a maximum Mach number variation within a 4-inch-high test rhombus of less than 1.6% at each Mach number tested in the range M = 1.3 to 4.0.

Final Contours

The contours of the nozzle as finally adjusted were measured with a vernier height gage and cast iron straightedge. The measurements, when plotted as y-coordinate displacements from the theoretical contours, revealed a small amount of waviness having maximum amplitude midway between jacks. This waviness, which is believed to be an unavoidable consequence of supporting a flexible plate by a finite number of jacks, was eliminated by fairing a smooth curve through the measured points for each nozzle block. These final faired contours are shown in Fig. 2 in the form of displacements from the theoretical contours. The coordinates of the final faired contours and those of the theoretical inviscid contours are tabulated in Reference 7.

Direct measurements of the curvature of the nozzle contours were made by means of the gage shown in Fig. 3. This gage, with the distances between the middle contact and the other two contacts set at 1/2-inch, reads directly one-quarter of the average curvature in the 1-inch interval. Measured values of the curvature of the contours are presented in Figs. 4 and 5 together with the curvature of the theoretical contours and of the faired contours.

Some of the curvature measurements plotted in Fig. 4 were made close to the edge of the flexible plate. Near each jack location these edge measurements depart from measurements made nearer the center, because the transverse curvature of the plate is restricted by the jack attachment, whose width is almost that of the plate.

IV. FLOW EVALUATION WITH FINAL CONTOURS

Atmospheric Stagnation Pressure

The flow produced by the final contours was evaluated at M = 1.27, 1.34, 1.45, and 1.5 by means of floor static-pressure measurements, and at M = 1.6, 1.9, 2.5, 3.2 and 3.8 by pitot pressure measurements with the five-prong pitot rake. For most of the pitot tests the rake was mounted in the vertical roll position, and measurements were taken at a fixed height above the floor at axial stations spaced $0.5\sqrt{M^2 - 1}$ inches apart. Since the pitot orifices are 1/2 inch apart vertically, this axial spacing placed the orifices at the intersections of a network of equally spaced Mach lines. The pitot pressure measurements were made with mercury manometry, while static pressures were measured with Meriam red oil. The manometers were clamped near the end of each run and their heights read immediately afterward. All the tests were made at dew-points below -25°F.

Higher Stagnation Pressure

A limited number of runs was made at stagnation pressures of from 2 to 6 atmospheres in order to assess the effect of Reynolds' number variation on the nozzle performance. Fig. 6 shows the nozzle installation for the higher pressure tests. These tests were made at Mach numbers 1.9 and 3.2. Pitot pressures were measured at the same points in the flow as at atmospheric stagnation pressure, using similar instrumentation. The static pressure in the settling chamber was measured by two 100-inch Meriam mercury manometers in series, and

converted to stagnation pressure through an experimental correction factor. Stagnation temperatures were recorded on a Brown recorder. Stagnation pressure was controlled manually by a Fischer valve which throttled the flow from about 400 psi to the desired stagnation pressure. The 400 psi air came, in turn, from a Foster reducing valve which was connected to a 3000 psi air storage tank. A bourdon-tube pressure transducer with an Atcotran pickup gave the operator a sensitive indication of stagnation pressure variations. The stagnation pressure variation during the ten seconds that the manometers were unclamped was usually less than 1/2%. The dewpoint of the air was always less than -25°F.

Data Reduction

Method. The pitot pressure data were reduced by a method based on an analysis given in Appendix D of Reference 7. The data, as mentioned above, were taken at the points of intersection of a network of equally spaced upward-and downward-running Mach lines. Disturbance waves between two adjacent Mach lines produced a change in pitot pressure. The values of this change were obtained as the difference in pitot pressure ratio between a point on one line and a point on the other line lying on the same crossing Mach line. These difference values for a given pair of Mach lines were averaged in such a way that each measurement, where more than one measurement was made at a point, was given equal weight. These average difference values were then used in a plot showing the variation of pitot pressure ratio along a Mach line crossing the disturbances. This was done for the variation along both upward and downward Mach lines, and then the two combined

by reflection, assuming a 0.2-inch boundary-layer reflection thickness, to give the pitot pressure variation along a complete Mach line from floor reflection surface to ceiling reflection surface. A curve was faired through these points, and from it were read values of the faired difference in pitot pressure ratio between adjacent Mach lines of the network, along a crossing Mach line.

From the faired values of the difference in pitot pressure ratio between Mach lines of the network, a set of faired values of pitot pressure ratio, one value for each point of the network, was constructed. This set of faired values was chosen so that the overall average of the differences, between faired and measured values at a point, equaled zero. These faired values are considered to be the best estimates of the true values at the points of measurement that can be deduced from all the data considered as a whole.

The pitot pressure ratios were converted to Mach numbers with the assumption of isentropic flow through the nozzle. A fixed position of the test rhombus was chosen as a compromise between best flow uniformity over the Mach number range and minimum nozzle length. At each Mach number the Mach number distributions along the sides of the rhombus at this location were integrated, and the average Mach number within the rhombus was obtained. The maximum plus and minus deviations from the average within the rhombus were then found. The same steps were followed to obtain the flow-angle deviation from the average.

Accuracy. An indication of the accuracy of the data reduction procedure is given in Fig. 7. This figure presents the standard deviation of the measured values from the faired (average) values as a function of Mach number. Also plotted for comparison is the expected standard deviation due to experimental error only, as determined by statistical analysis of repeat data. These values of standard deviation are in terms of pitot pressure ratio. For convenience in converting to Mach number or flow angle the magnitudes of the deviation in pitot pressure ratio associated with 0.1% change in Mach number and 0.05° change in flow inclination are also shown.

Another comparison between the measured values of pitot pressure ratio and the faired values is presented in Fig. 8. This typical figure shows the faired pressure-ratio variation along Mach lines through the points of measurement, together with the measured values. The scales have been stretched linearly for ease of plotting.

Two Dimensionality. The results given above were obtained in the vertical center plane of the tunnel and reduced by a process which assumes two-dimensional flow. The validity of this assumption was checked by measurements made with the five-prong pitot rake in a horizontal attitude. At most locations of the rake the agreement of the five measurements was very good. The greatest deviation between measurements along any transverse line was about 0.2% in Mach number. This occasional slight non-two-dimensionality may account for the increase of the standard deviation over that given by the experimental errors in Fig. 7.

Details. Representative details of some steps in the data evaluation process are shown in Figs. 9 and 10. Fig. 9 shows the static-pressure distribution along the floor of the test section at M = 1.27, 1.34, 1.45, and 1.51. As the static-pressure measurements were relative, the average Mach number values shown here were obtained by extrapolation of pitot pressure measurements at M = 1.6 and above. Each curve covers one complete cycle of the pressure variation along the floor.

Fig. 10 shows the variation of pitot pressure ratio at M = 1.93 along the exit Mach line (the upward-running Mach line intersecting the upper contour at the nozzle end). In this figure the difference in value between adjacent points of like symbol represents the average of the pitot-pressure ratio changes measured between Mach lines which cross the exit Mach line at the height shown. The points at the ends of a series of like symbols were not given as much weight in fairing as those nearer the middle, since they represent the averages of only a few measurements.

The Mach number variation along the nozzle exit Mach line for each of the nine Mach number settings is shown in Fig. 11.

Results

Flow Uniformity. The main calibration results with the final contours are summarized in Fig. 12 and representative details are given in Figs. 13 to 16. Fig. 12 shows the maximum plus and minus deviations of Mach number or flow angle from the average, within a

4-inch-high test rhombus centered at the nozzle exit (end of curved part of upper contour). For this rhombus the horizontally projected throat-to-test-rhombus distance varies between 6.4 and 8.8 times the rhombus height of 4 inches for Mach numbers from about 1.5 to 4.0.

As shown in Fig. 12, the Mach number deviation from the average within the test rhombus is less than $\pm$ 0.9% for each Mach number tested in the range M = 1.3 to 4.0. The flow angle deviation is less than $\pm$ 0.5°. The highest Mach number obtained, due to mechanical limitations in the lower block traversing mechanism, was 3.84, but the trend of the data suggests that a considerable increase in Mach number might be realized before the above deviation limits would be exceeded.

Figs. 13 and 16 present details of the flow along the edges of the test rhombus at four Mach numbers from 1.27 to 3.84. It should be noted that the Mach number (or flow angle) at any point within the test rhombus can be easily determined by moving any of the edge curves (in the appropriate diagram) parallel to itself to the position in question, keeping the ends of the curve on the adjacent edge curves. This process is illustrated in Fig. 14, where the Mach number deviation at point D is determined.

The change of average Mach number in the test rhombus with lower block axial position is presented in Fig. 17 together with the theoretical variation based on the measured throat-to-test section area ratios.

Reynolds' Number Effect. The data from the tests at stagnation pressures of from 2 to 6 atmospheres are presented in Fig. 18. Comparison of the plotted points with the solid curve, representing the atmospheric pressure results, shows that the difference in Mach number distribution in the test section, due to a sixfold increase in Reynolds' number, is within the measuring accuracy.

V. DISCUSSION

Nozzle Coordinates

The final faired coordinates determined by this program (and tabulated in Reference 7) are recommended for use in wind tunnels designed for the Reynolds' number range of the present tests. These recommended contours differ from the tested contours by amounts up to 0.004 inches, but the difference is such that unnecessary waviness between jacks in the actual nozzle is eliminated in the final faired coordinates. It is therefore believed that these coordinates should give flow uniformity as good as, or better than, that of the actual nozzle (Fig. 12).

Contour Tolerances

It can be shown (Reference 7, Appendix E) that flow-angle errors greater than $\pm\ \Delta\alpha$ degrees due to contour defects will be avoided if the coordinates of the nozzle are accurate to within $\pm\ 0.02\ \Delta\alpha^{\circ}$ inches, and if certain tolerances on short wavelength waviness are met. These waviness tolerances can be stated in terms of the reading of a curvature gage of the type shown in Fig. 3. Such a gage reads a value G in inches given in terms of the coordinates as

$$G = \frac{\Delta^2 y}{\left[1 + \left(\frac{\Delta y}{\Delta x}\right)^2\right]^{3/2}}$$

where Δx equals the distance in inches between the center contact and each of the two outer contacts, Δy is the change in y, in inches,

associated with Δx, and $\Delta^2 y$ is the difference between the Δy's of the two adjacent Δx intervals spanned by the gage (second difference). For a given gage length and nozzle size, the correct values of G may be computed from the above equation and the nozzle coordinates.

If the readings of a 1-inch curvature gage do not depart from the correct values computed from the above equation by more than $\pm$ 0.014 $\Delta\alpha^\circ$ inches, then the test-section flow should be free of flow-angle errors greater than $\pm$ $\Delta\alpha$ degrees due to contour defects having sinusoidal wavelengths greater than 1.55 inches. If, in addition, the readings of a 1/4-inch curvature gage agree with the correct values to within $\pm$ 0.004 $\Delta\alpha^\circ$ inches, then flow-angle errors due to all defects having wavelengths greater than 0.4 inches will be less than $\pm$ $\Delta\alpha$ degrees.

Scale Effects

The final faired contours should produce satisfactory flow for nozzle sizes and stagnation conditions represented by $.0228 < h\ p_o/T_o^{1.26} < .160$, where p_o is the stagnation pressure in psia, T_o is the stagnation temperature in degrees Rankine, and h is the vertical distance in inches between coordinate origins of the two blocks (h = 4.37 inches for the present nozzle). At any given Mach number the Reynolds' number is approximately proportional to the parameter $h\ p_o/T_o^{1.26}$ (assuming the viscosity $\mu = \mu_o\ (T/T_o)^{.76}$). For the above range of this parameter, the corresponding Reynolds' numbers based on h are Re = 1.68 to 11.8×10^6 at M = 1.27 and Re = .55 to 3.86×10^6 at M = 3.84.

For combinations of stagnation conditions and nozzle size outside the above range, it may be desirable to alter the present contours to compensate for the change in boundary-layer thickness. One approximate way of doing this would be to reduce the lower block y-values and increase those of the upper block by the difference between boundary-layer corrections computed at the old and new Reynolds' numbers, for some arbitrary Mach number.

VI. DIFFUSER PERFORMANCE

The nozzle model was originally equipped with an adjustable supersonic diffuser. The flow through this diffuser was bounded on the bottom by a flat plate extension of the lower nozzle block, on the sides by parallel flat walls, and on the top by two flat plates hinged together. The upstream plate was 25 inches long; the downstream plate, 37 inches. The hinge point between these plates could be lowered, reducing the angle between the plates to less than 180°, and forming a throat. This throat was 37 inches downstream of the nozzle exit.

The entrance cross section of the adjustable diffuser was 4 inches wide and from 4- to 5-1/2 inches high, depending on the nozzle configuration. The exit of the adjustable diffuser was 4 by 5 inches. A 5-foot-long transition section continued the subsonic diffusion to the 8-inch-diameter butterfly valve.

The performance of the adjustable diffuser described above, in conjunction with the empty tunnel with jacks set for the theoretical contours, was determined by measuring the vacuum tank pressure at the moment of flow break-up. The resulting overall pressure ratios required to maintain supersonic flow are shown in Fig. 20 for two conditions: (1) diffuser throat wide open, and (2) diffuser throat closed to optimum position after starting. Minimum diffuser throat-to-test section area ratios for starting and for maintaining flow are shown in Fig. 21.

The overall pressure ratios of Fig. 20 with diffuser throat closed to optimum position after starting are somewhat higher than those of a pitot tube. It is probable that this performance could be improved by modifications of the adjustable diffuser geometry.

VII. CONCLUSIONS

1. A sliding-block variable Mach number wind-tunnel nozzle for the Mach number range 1.3 to 4.0 has been developed, by means of iterative characteristic theory with experimental corrections. Calibration of the flow in this nozzle has revealed the following:

(a) The Mach number deviation from the average within a test rhombus is less than $\pm$ 0.9% throughout the Mach number range 1.3 to 4.0.

(b) In this range the flow angle deviation from the average within a test rhombus is less than $\pm$ 0.5°.

(c) The horizontally projected throat-to-test rhombus center distance is 8.8 times the test rhombus height at the highest Mach number.

(d) A six-fold increase in Reynolds' number has negligible effect on the flow uniformity.

(e) The overall pressure ratios required to run the nozzle with an adjustable diffuser are about the same as those required by symmetrical nozzles with fixed diffusers.

2. An economical, general purpose, variable Mach number supersonic nozzle can be designed from the results of this program provided the length of the nozzle can be accommodated.

3. The nozzle appears suitable for the simulation of time-variable Mach number conditions.

4. Additional work on this nozzle could lead to an extension of the Mach number range into the hypersonic and transonic regimes.

REFERENCES

1. Allen, H. Julian, The Asymmetric Adjustable Supersonic Nozzle for Wind Tunnel Application. NACA TN 2919. March, 1953.

2. Syvertson, Clarence A. and Savin, Raymond C., The Design of Variable Mach Number Asymmetric Supersonic Nozzles by Two Procedures Employing Inclined and Curved Sonic Lines., NACA TN 2922, March, 1953.

3. Burbank, Paige B., and Byrne, Robert W., The Aerodynamic Design and Calibration of an Asymmetric Variable Mach Number Nozzle with a Sliding Block for the Mach Number Range, 1.27 to 2.75, NACA TN 2921. April, 1953.

4. Murphy, J. S., and Buning, H., Theory and Design of a Variable Mach Number Corner Nozzle. University of Michigan. WTM 221. April-December, 1951.

5. Liepman, H. P., An Analytic Design Method for a Two-Dimensional Asymmetric Curved Nozzle. University of Michigan, June, 1953. Also Jour. Aero, Sci., Vol. 22, No. 2, 1955 p.

6. Liepman, H. P., Murphy, J. S., and Nourse, J. H., A Physical Description of a Variable-Mach-Number 4- by 4-Inch Pilot Corner Nozzle. University of Michigan, WTM 246., December, 1953.

7. Amick, J. L., Liepman, H. P., and Reynolds, T. H., Development of a Variable Mach Number Sliding Block Nozzle and Evaluation in the Mach Number Range 1.3 to 4.0, WADC Techn. Report No. 55-88, March, 1955.

8. Haefeli, Rudolph C., Use of Fences to Increase Uniformity of Boundary Layer on Side Walls of Supersonic Wind Tunnels, NACA RM E52E19, July, 1952.

9. Tucker, Maurice, Approximate Calculation of Turbulent Boundary Layer Development in Compressible Flow. NACA TN 2337. April, 1951.

NOMENCLATURE

G	Curvature gage reading
h	Distance between x-axes of upper and lower contours (Test section height)
M	Mach number
p	Static pressure
p_o	Stagnation pressure
p'_o	Pitot pressure
R	Radius of curvature
Re	Reynolds' number
T	Temperature
T_o	Stagnation temperature
x, y	Coordinates
α	Flow angle
Δ	Small, finite increment
σ	Standard deviation
μ	Coefficient of viscosity
μ_o	Stagnation coefficient of viscosity

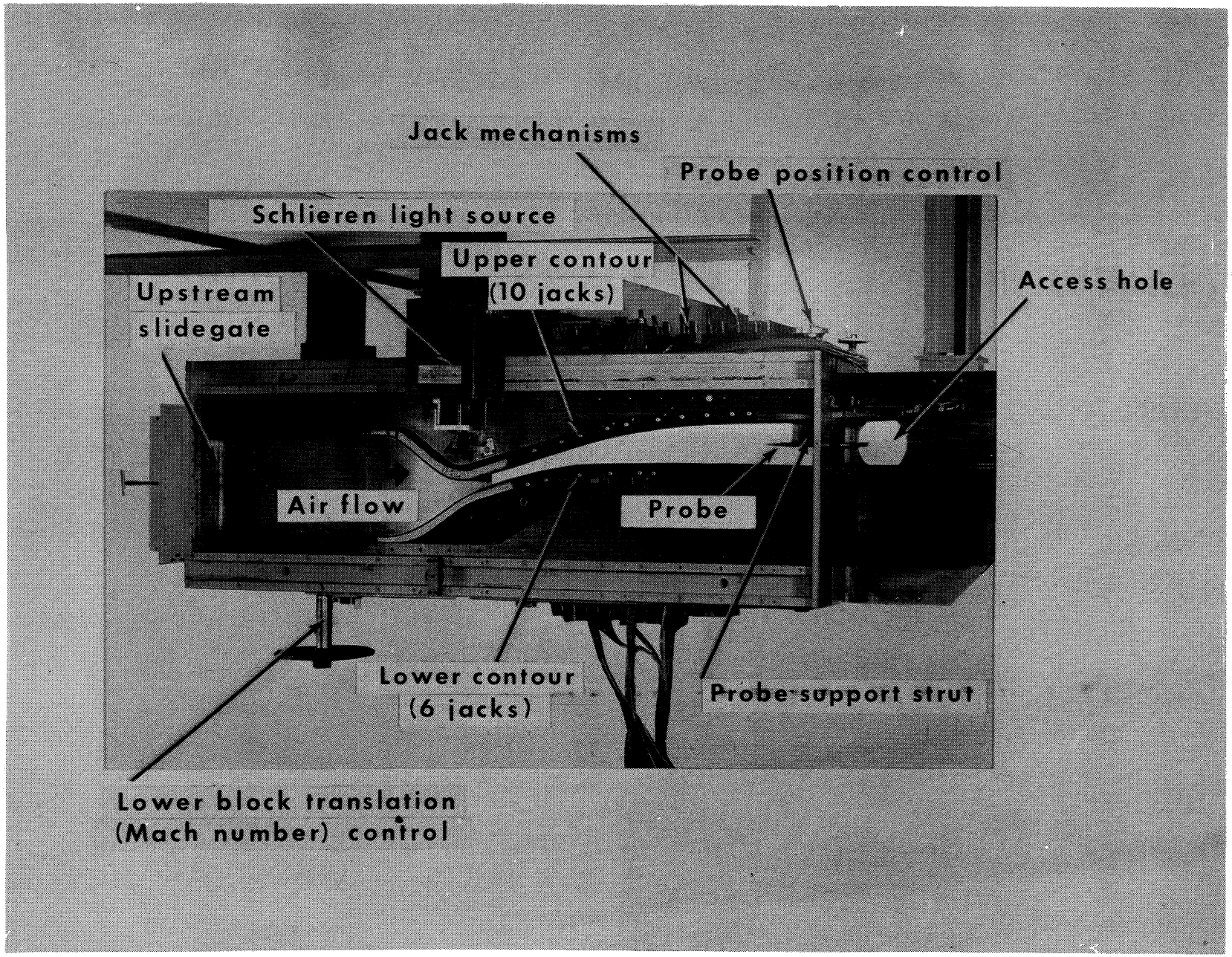

Fig. 1 View of Nozzle With One Side Removed

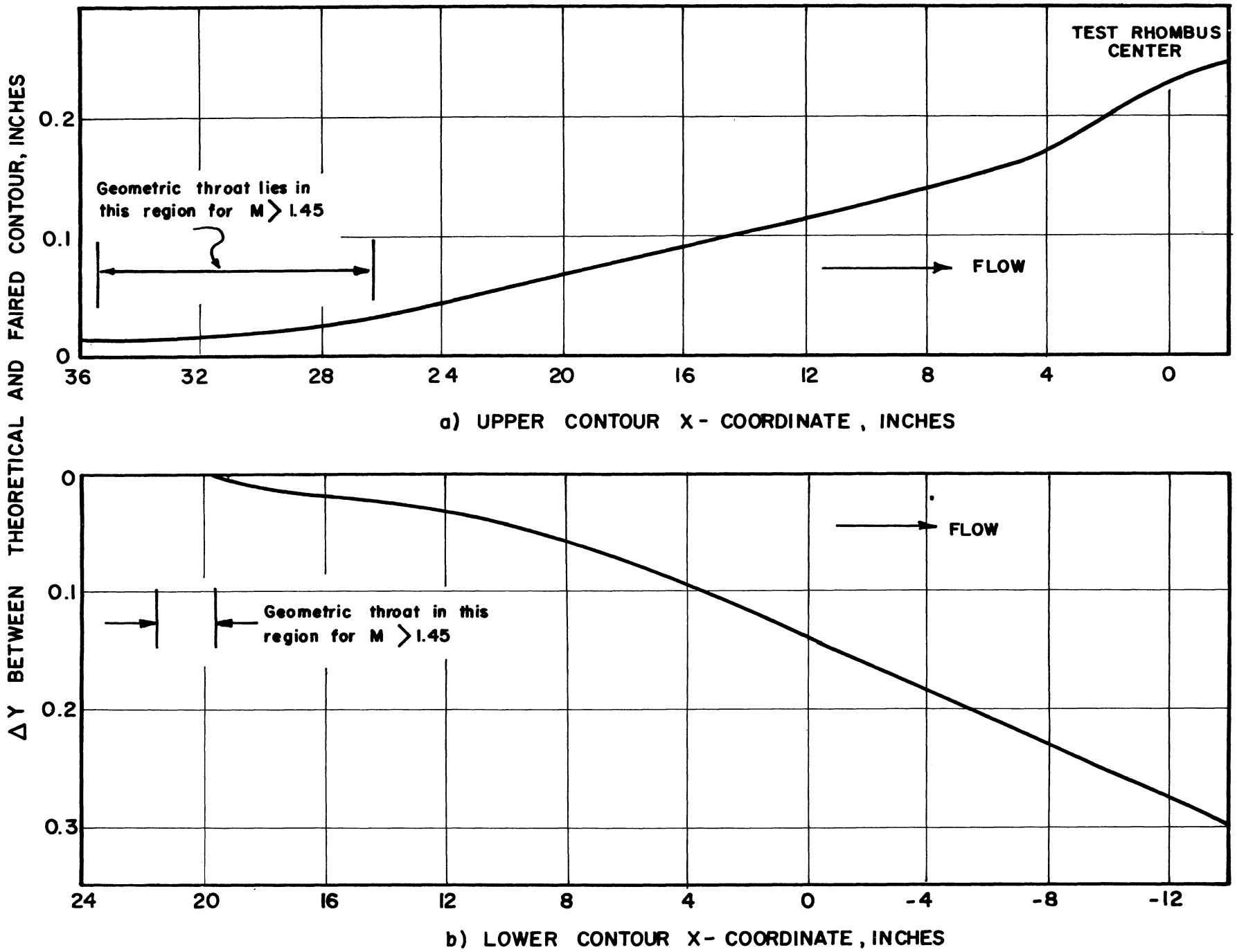

Fig. 2 y-coordinate Difference Between Faired and Theoretical Contours

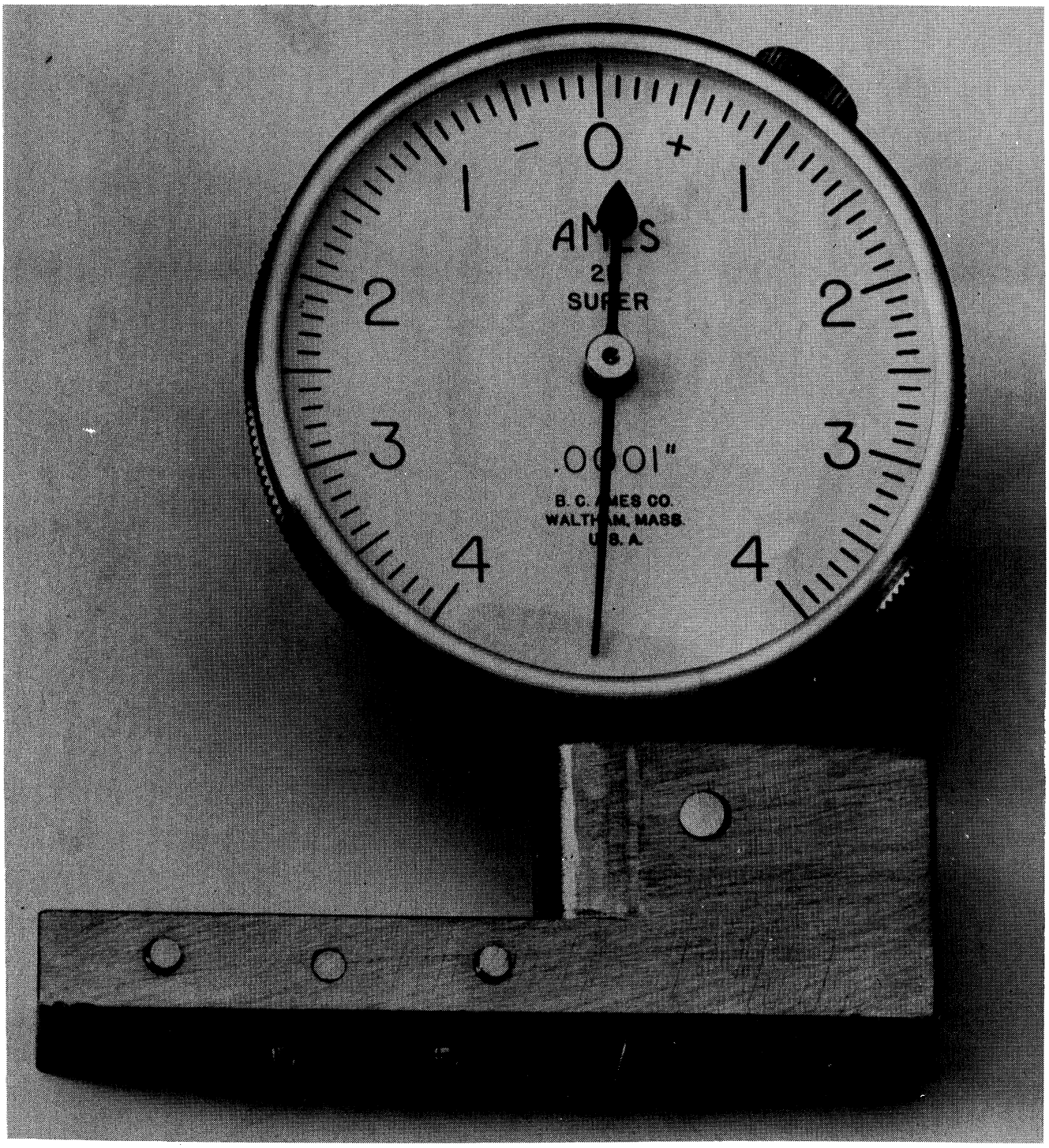

Fig. 3 Curvature Gage

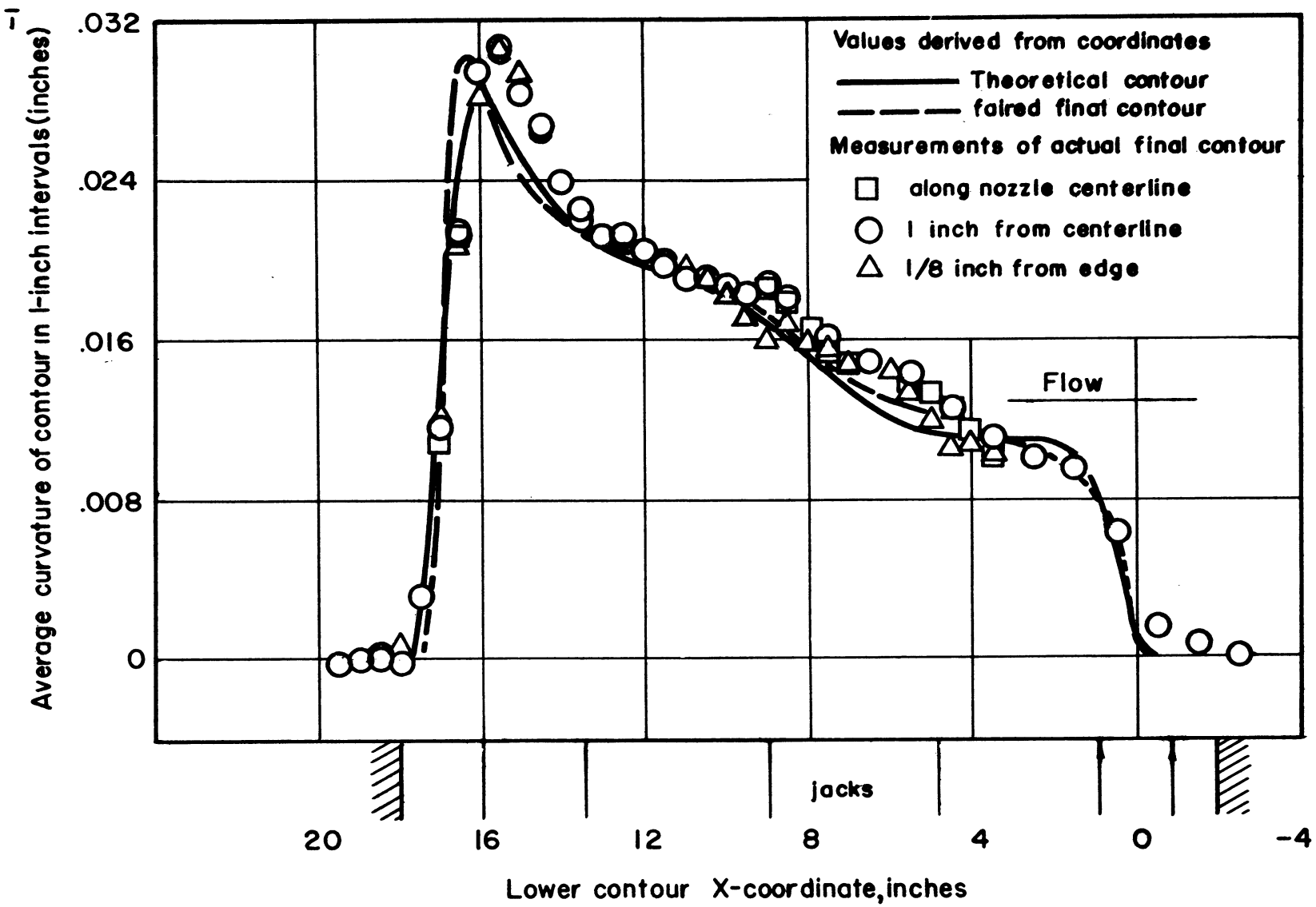

Fig. 4 Average Curvature of Lower Contour in 1-Inch Intervals

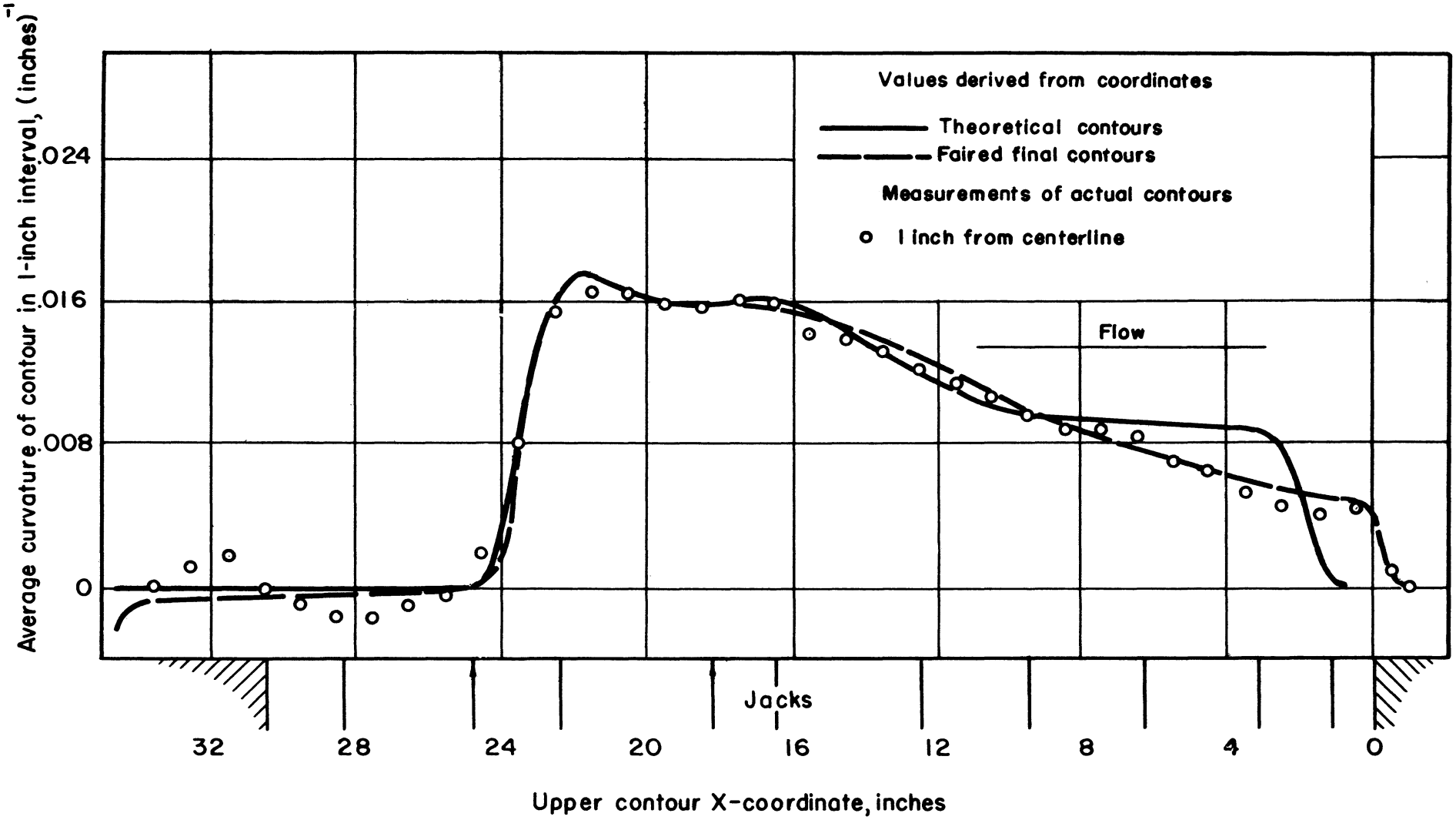

Fig. 5 Average Curvature in 1-Inch Intervals for Upper Contour

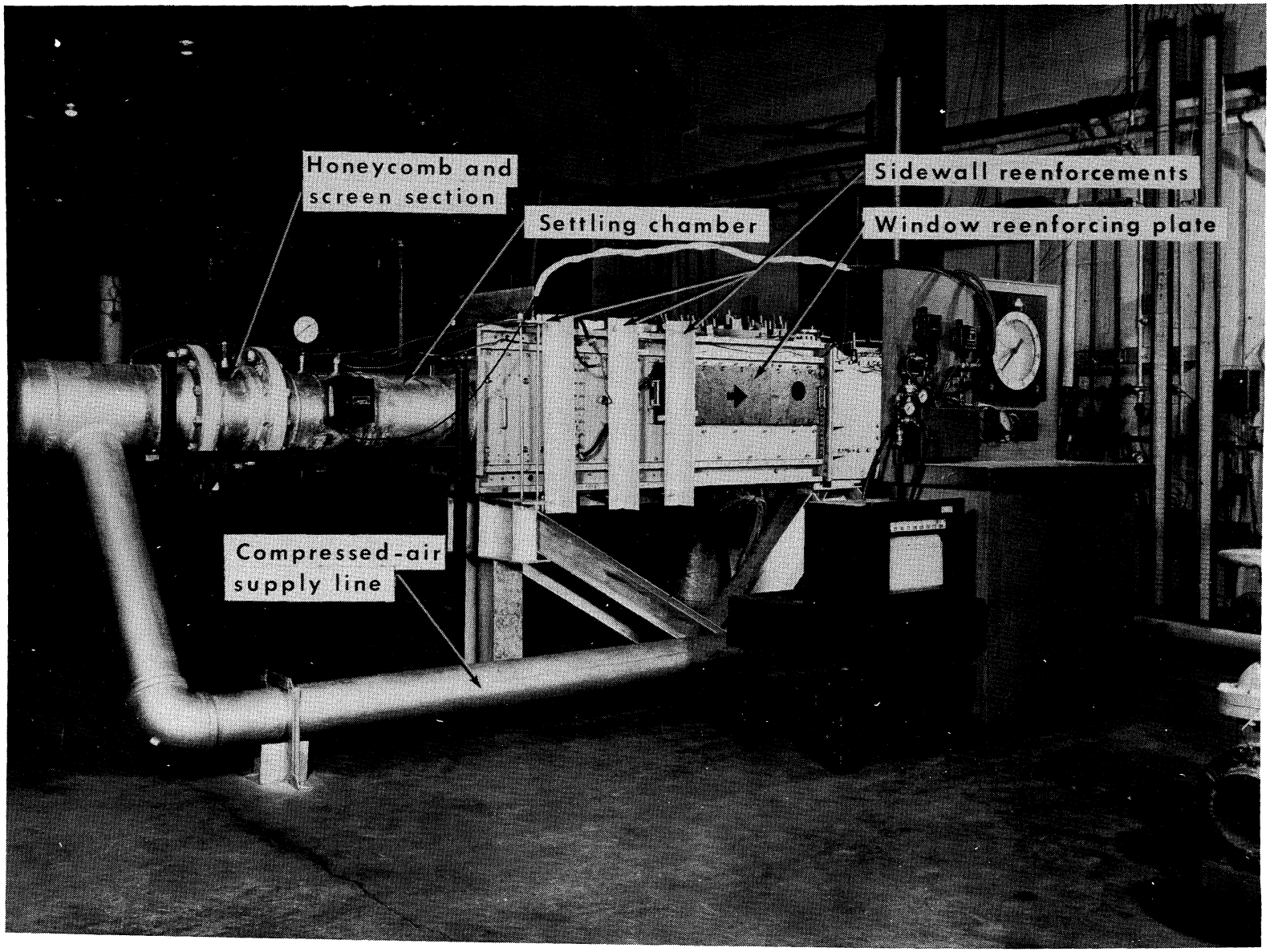

Fig. 6 Nozzle Installation for Higher Stagnation Pressure Tests

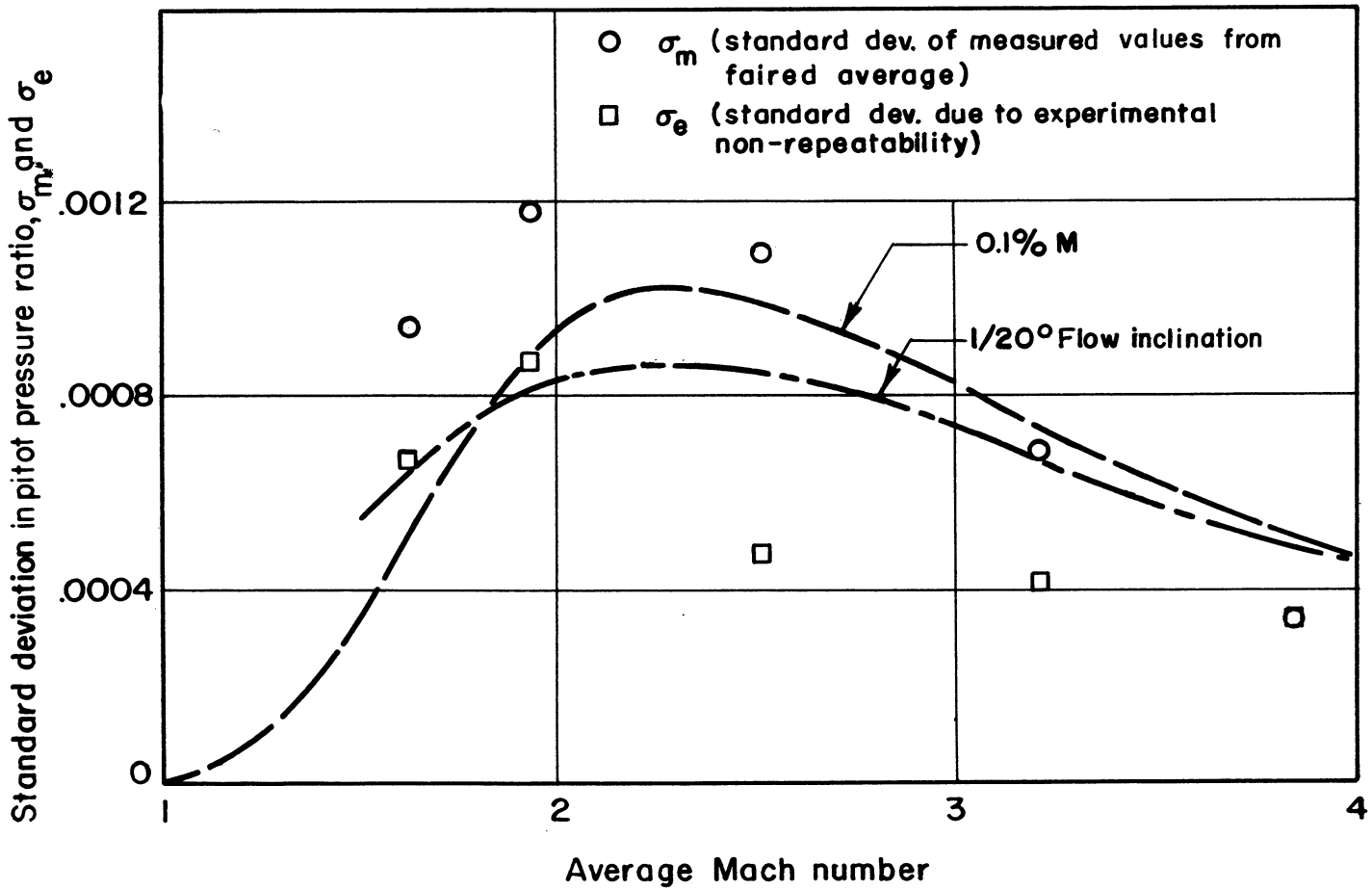

Fig. 7 Standard Deviation of Pitot Pressure Measurements From Faired Values. Tests at Atmospheric Stagnation

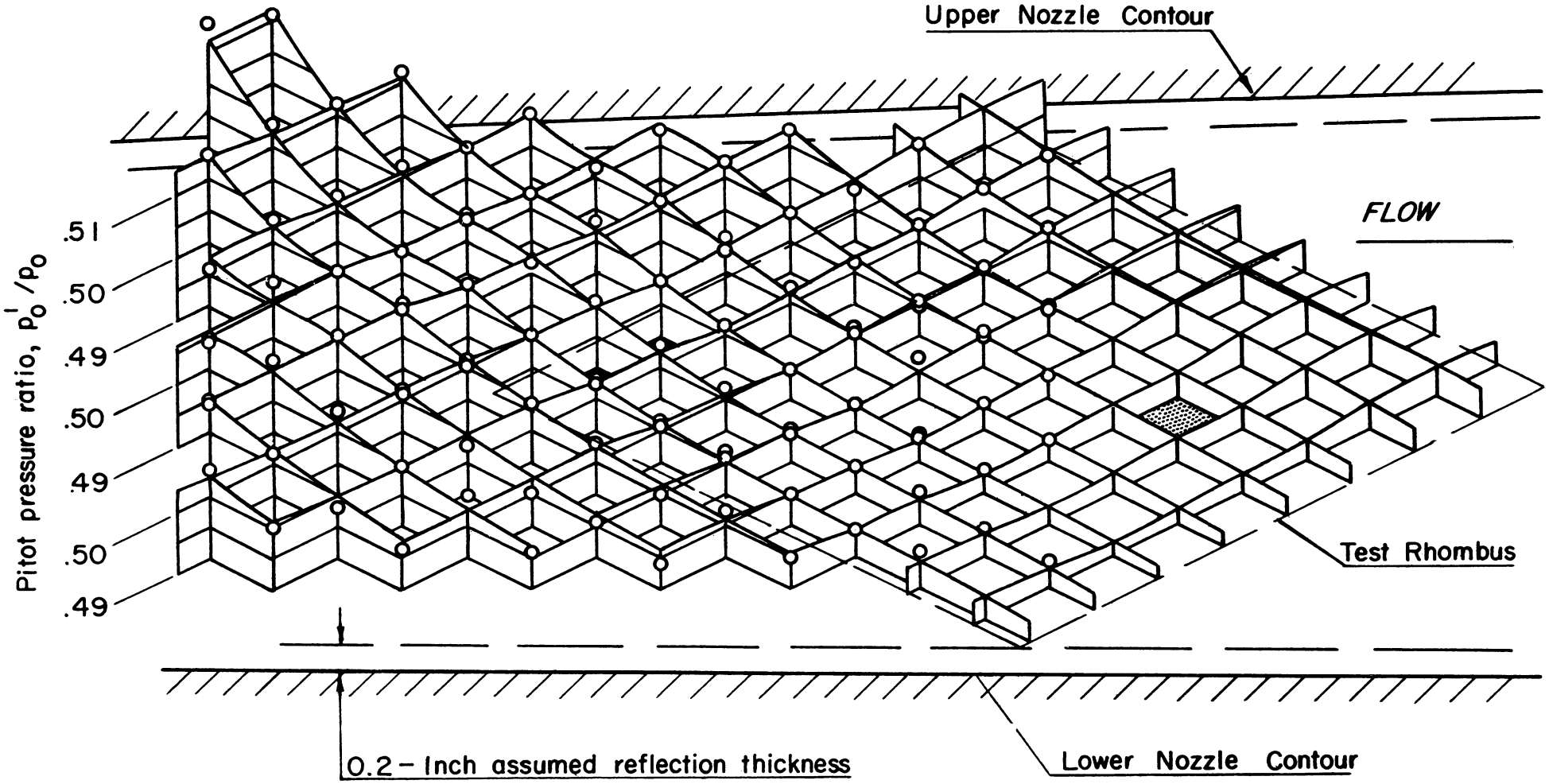

Fig. 8 Comparison of Faired Pitot-Pressure Distribution with the Data Points. M = 2.51. Atmospheric Stagnation

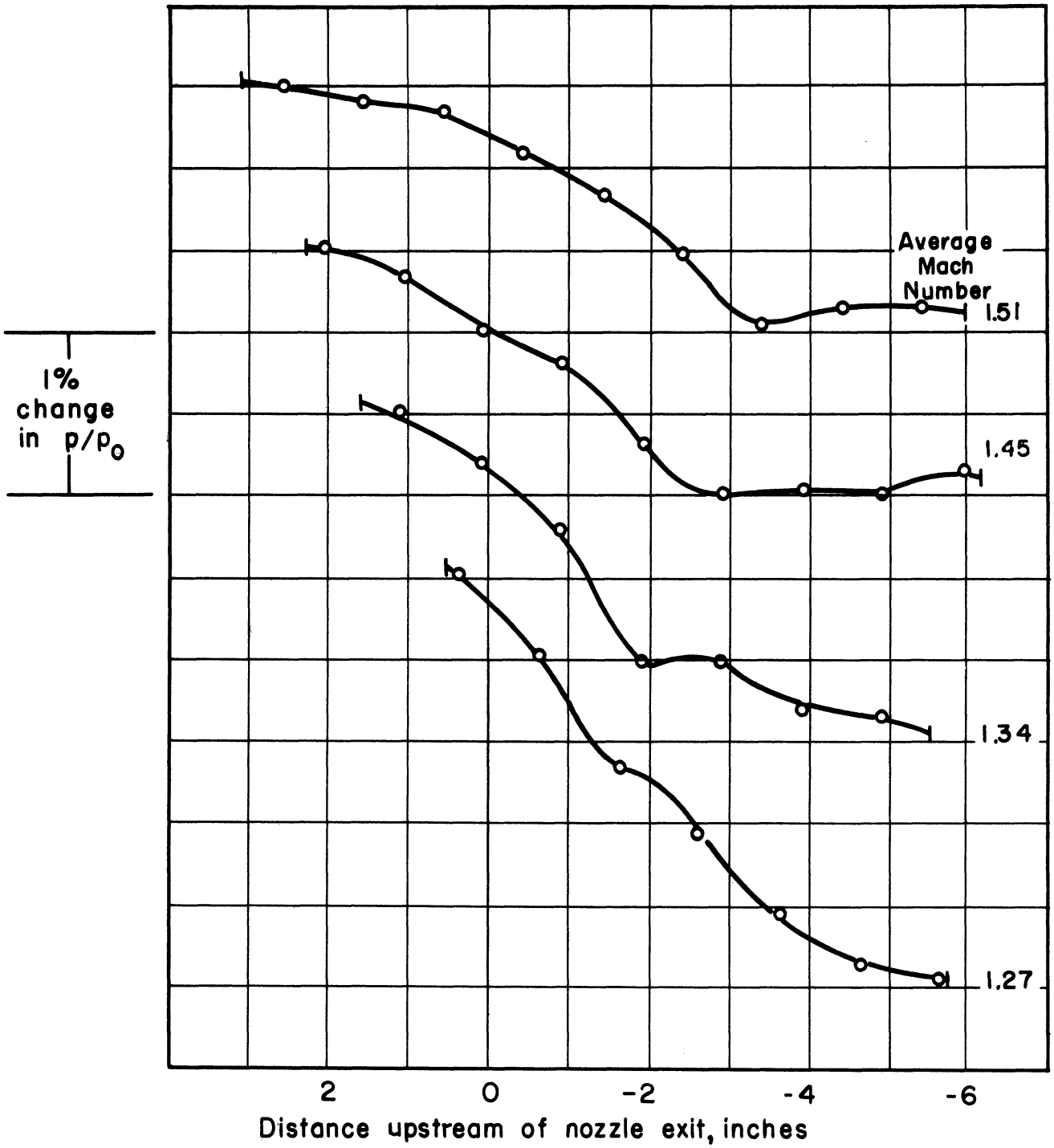

Fig. 9 Static Pressure Distribution along Floor of Test Section at M = 1.27, 1.34, 1.45, and 1.5. Atmospheric Stagnation

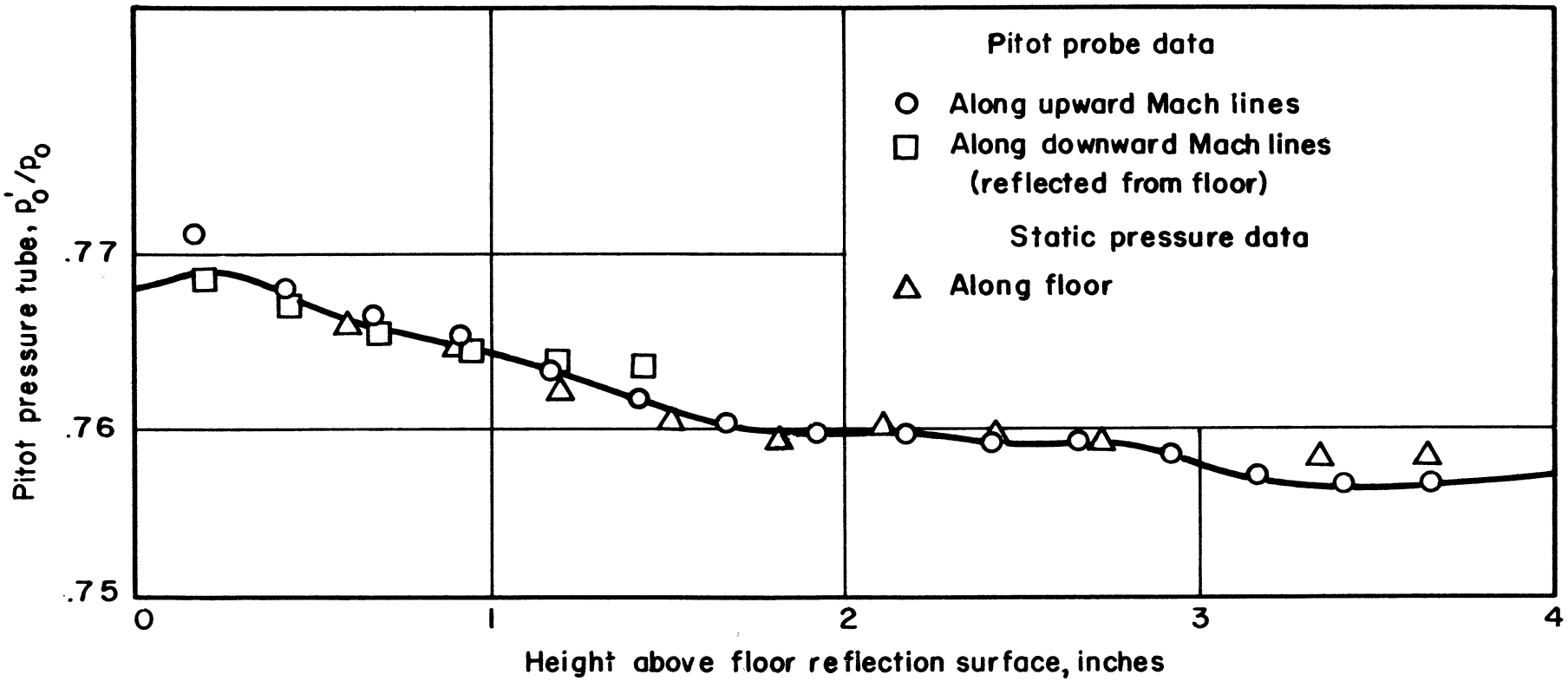

Fig. 10 Pitot-Pressure Ratio Distribution along Exit Mach Line at M = 1.93. Atmospheric Stagnation

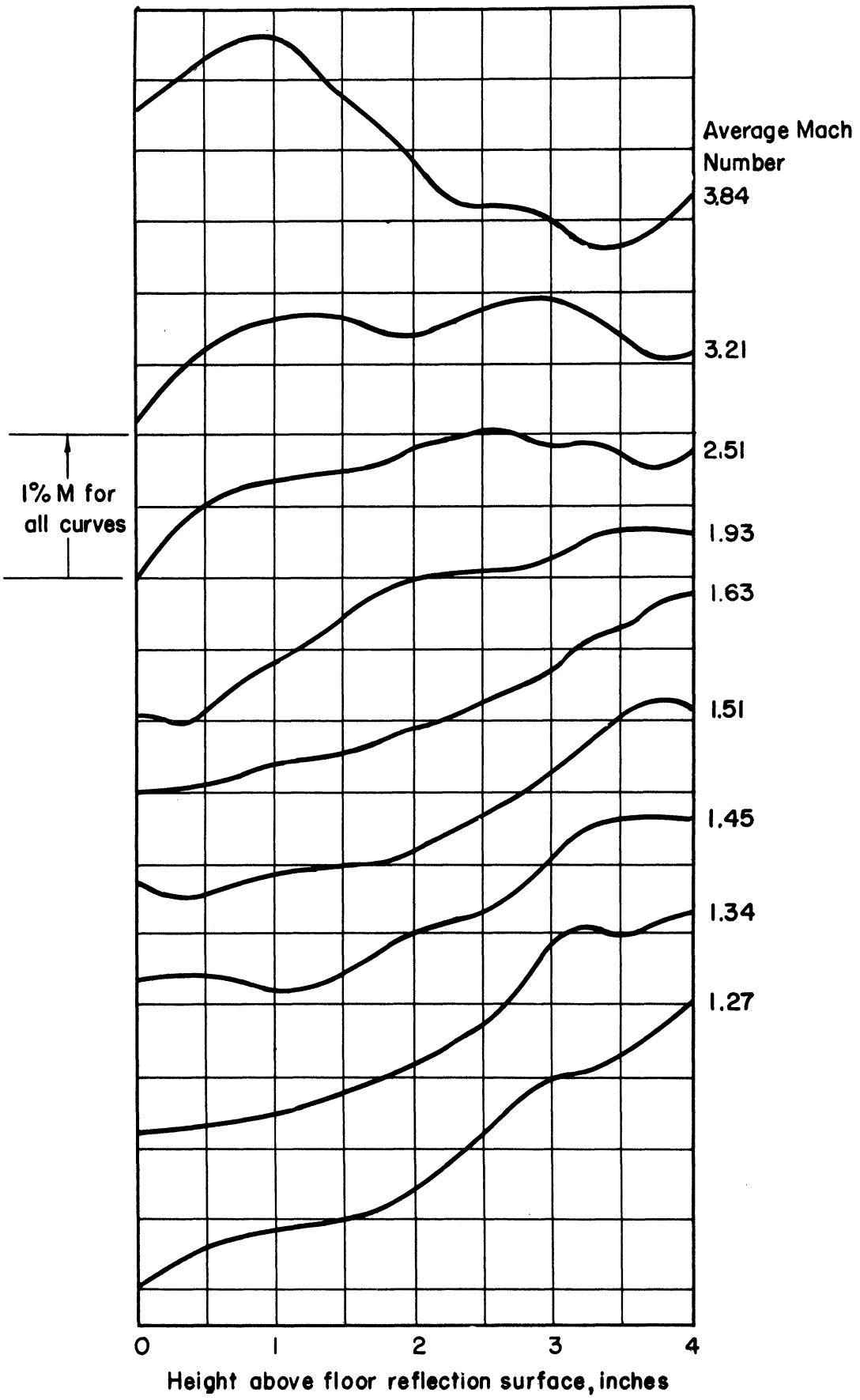

Fig. 11 Mach Number Distribution along Nozzle Exit Mach Line

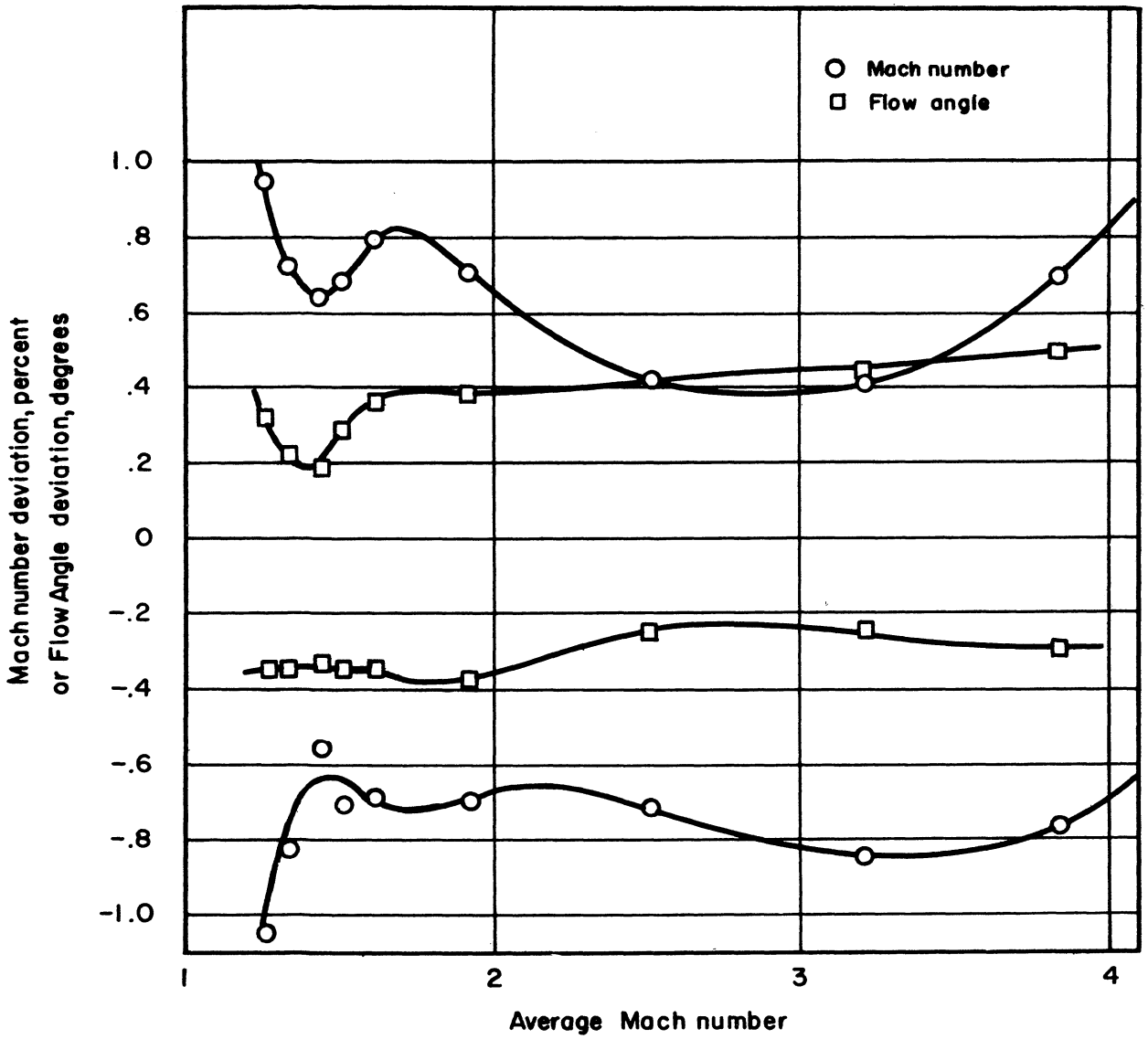

Fig. 12 Maximum Deviations of Mach Number and Flow Angle from Average Within a 4-Inch High Test Rhombus Centered at the Nozzle Exit.

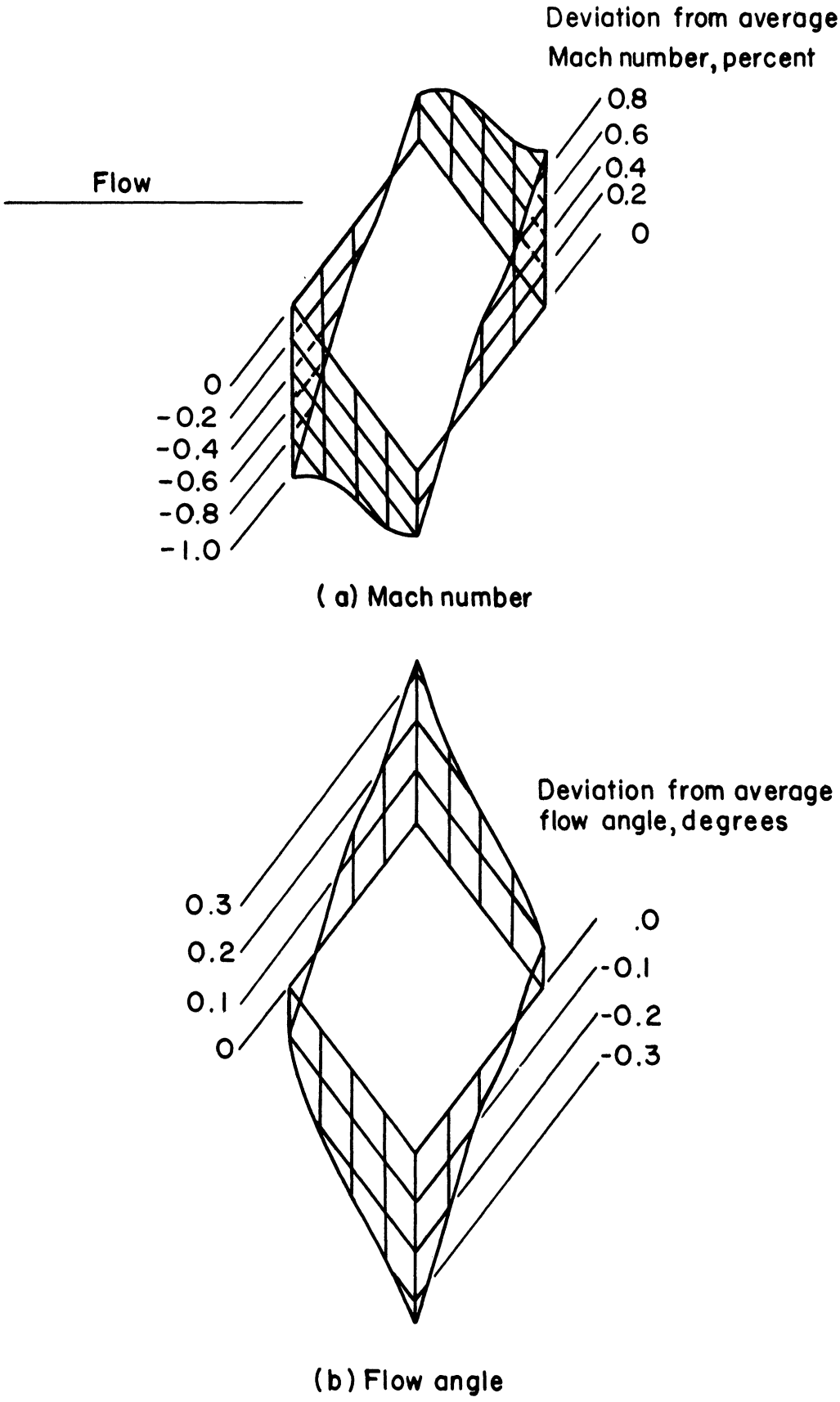

Fig. 13 Mach Number and Flow-Angle Variation Along Test-Rhombus Perimeter. M = 1.27

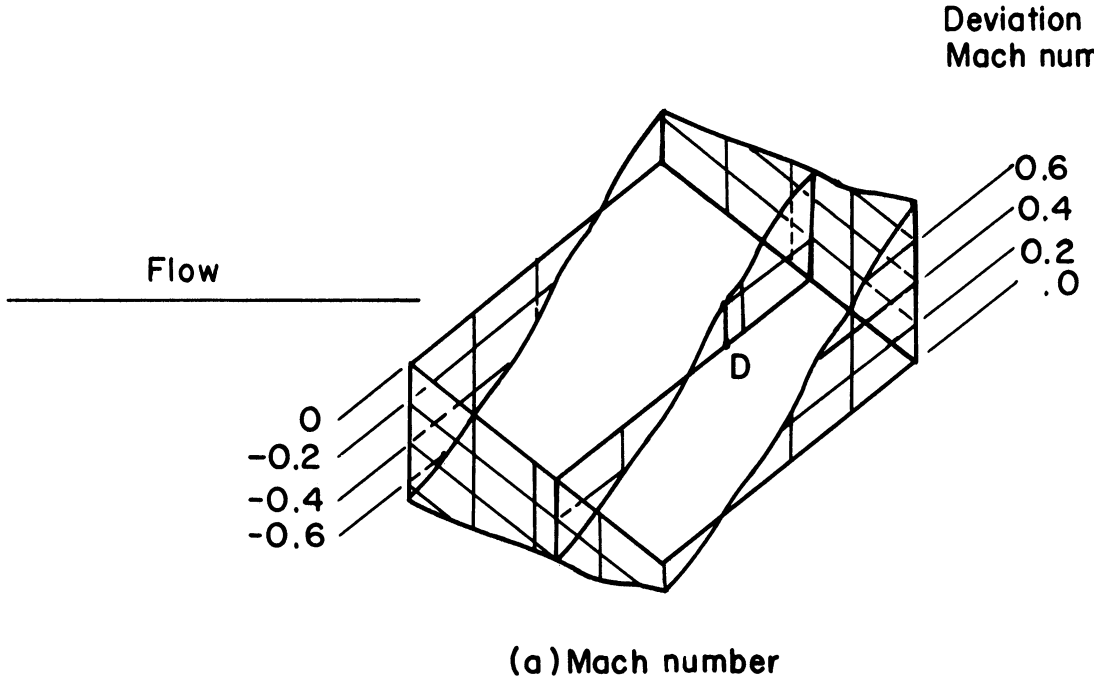

(a) Mach number

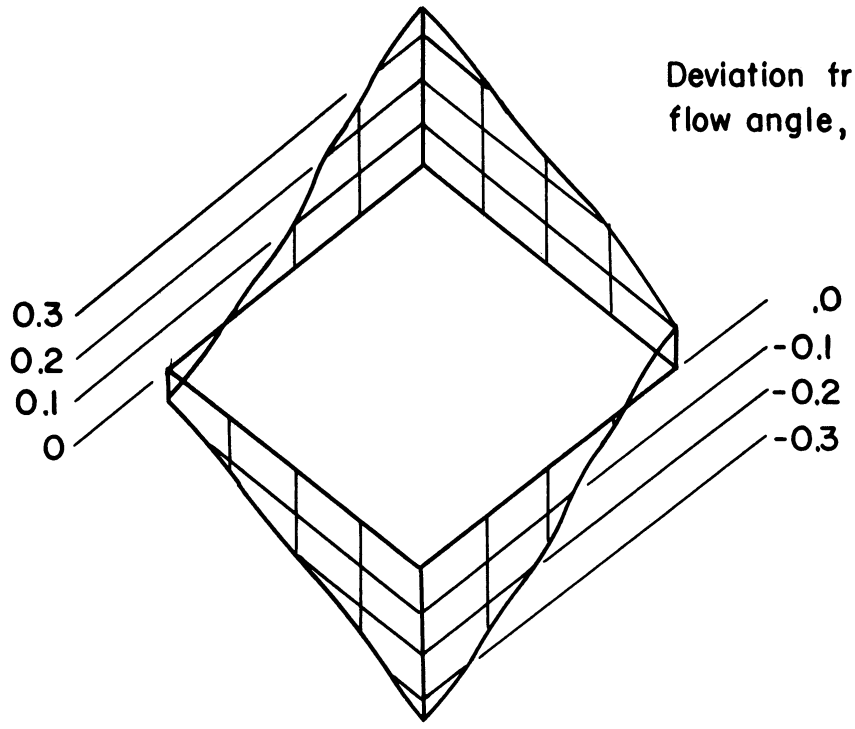

(b) Flow angle

Fig. 14 Mach Number and Flow-Angle Variation Along Test-Rhombus Perimeter. M = 1.63.

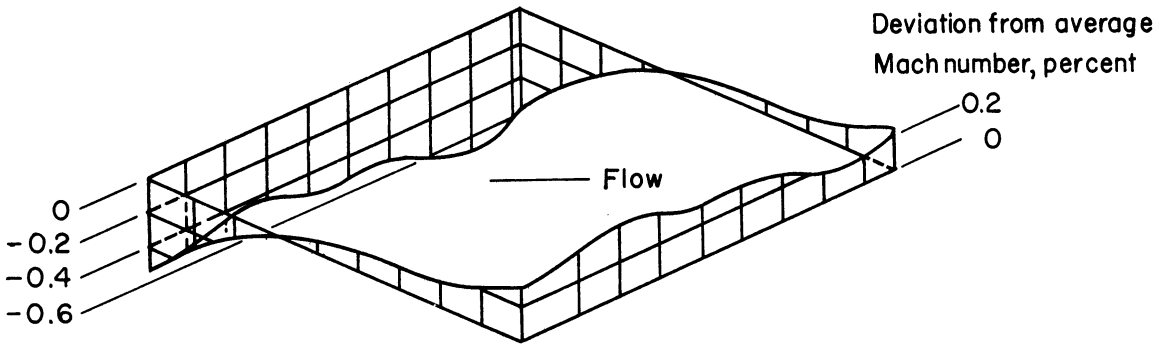

(a) Mach number

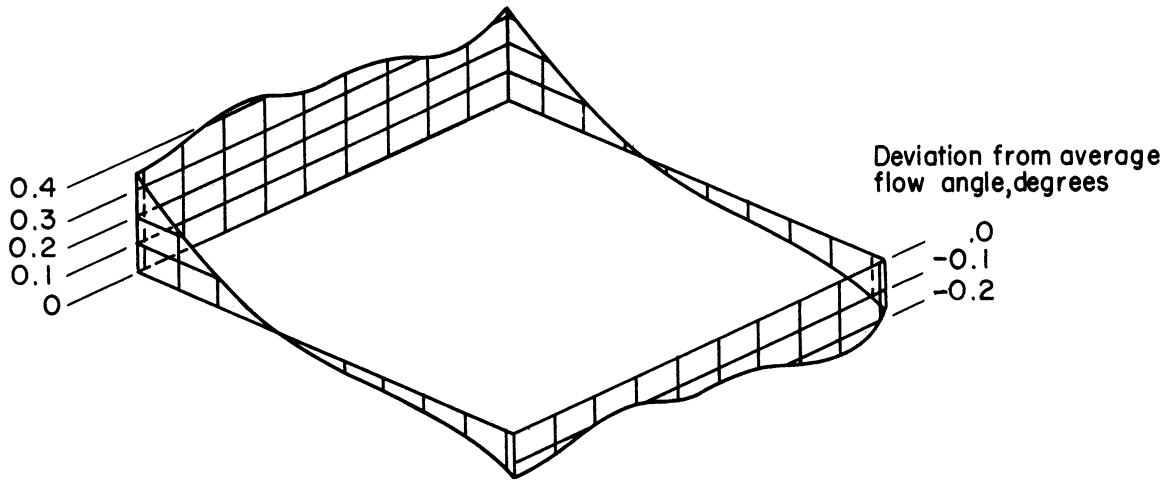

(b) Flow angle

Fig. 15 Mach Number and Flow-Angle Variation Along Test-Rhombus Perimeter. M = 2.51

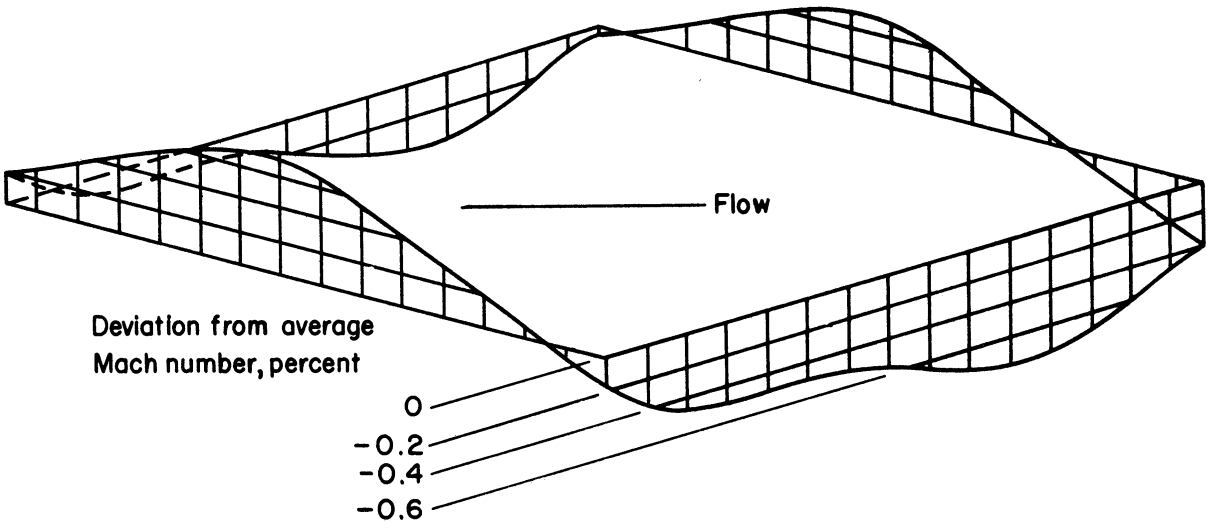

(a) Mach number

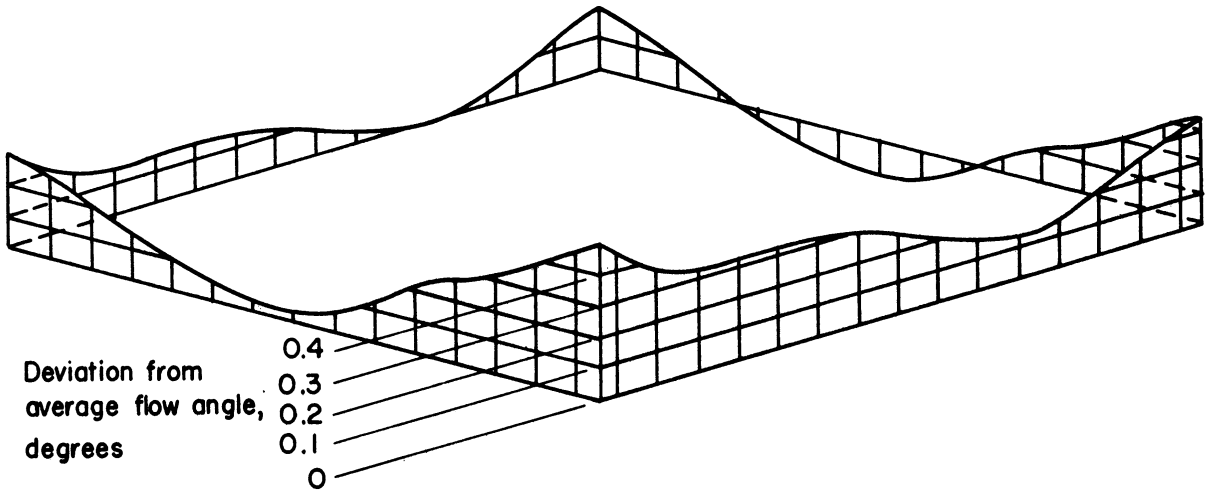

(b) Flow angle

Fig. 16 Mach Number and Flow-Angle Variation Along Test-Rhombus Perimeter. M = 3.84

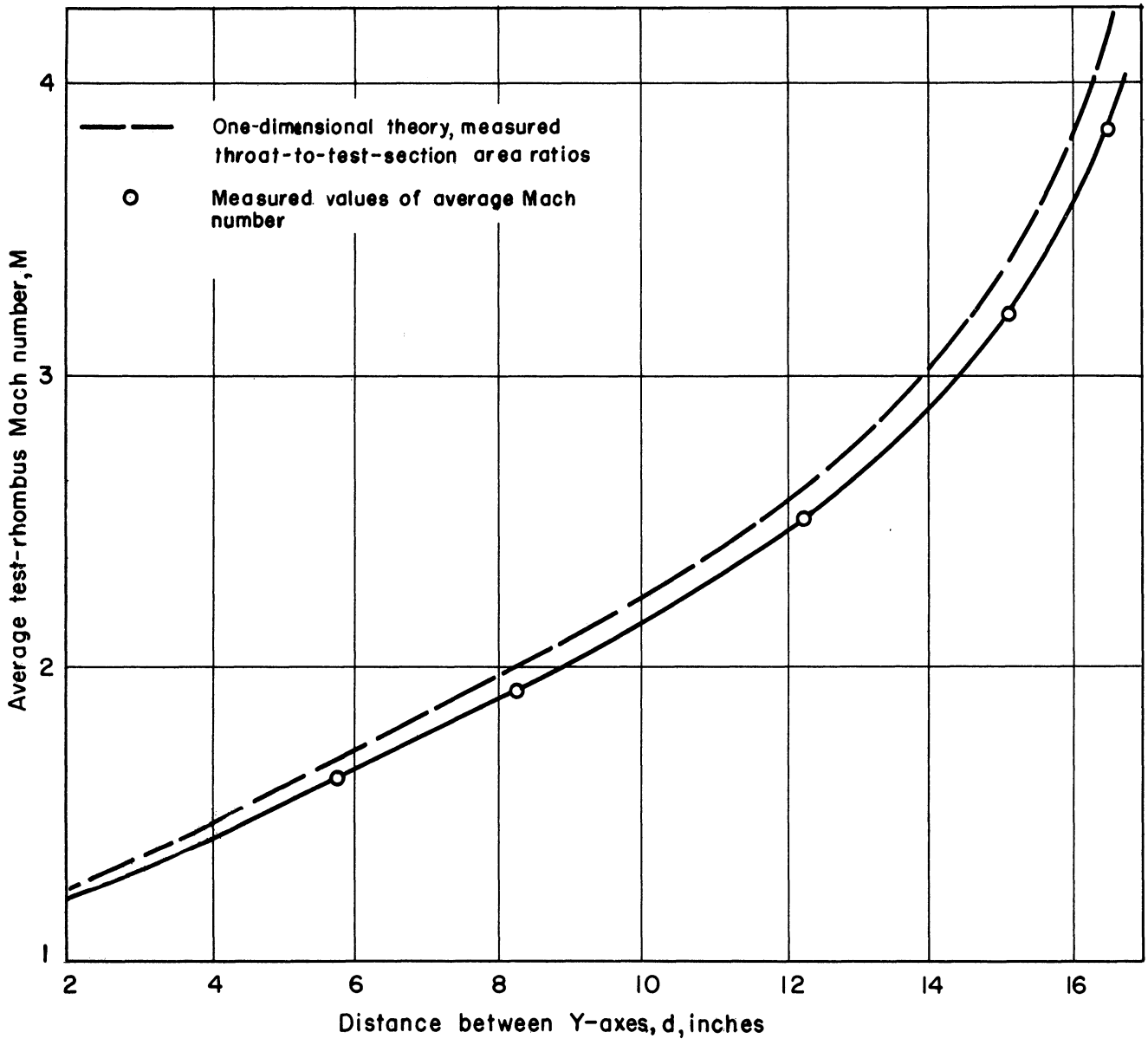

Fig. 17 Relationship Between Lower-Block Axial Setting and Average Test-Rhombus Mach Number

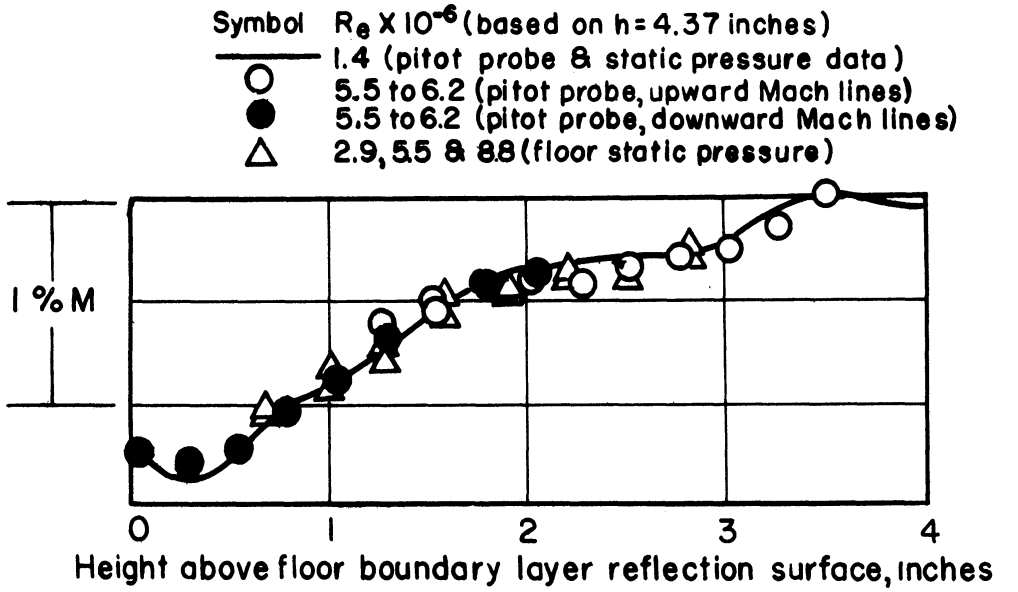

(a) M = 1.93

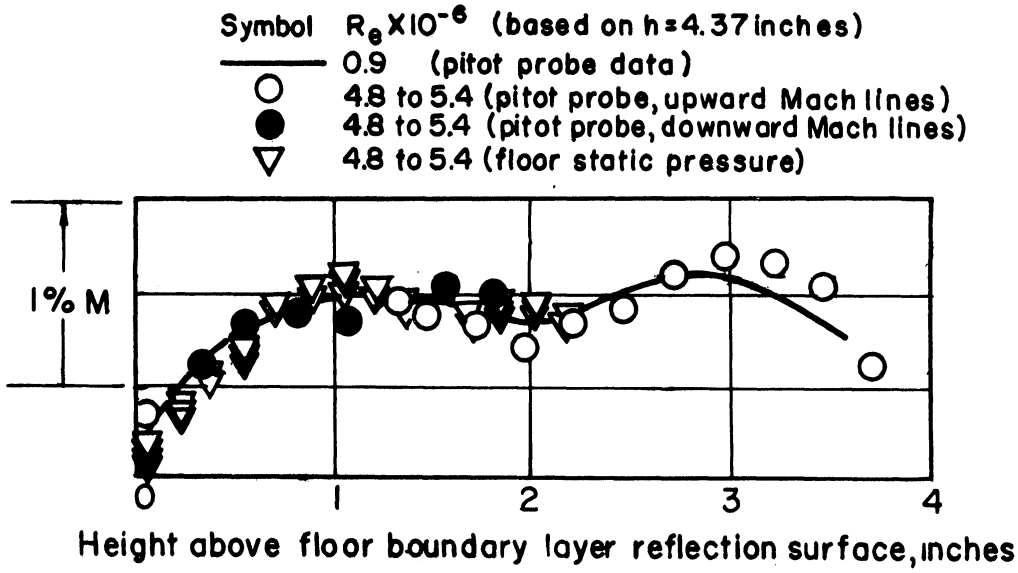

(b) M = 3.21

Fig. 18 Mach Number Variation Along Exit Mach Line at Higher Reynolds' Numbers

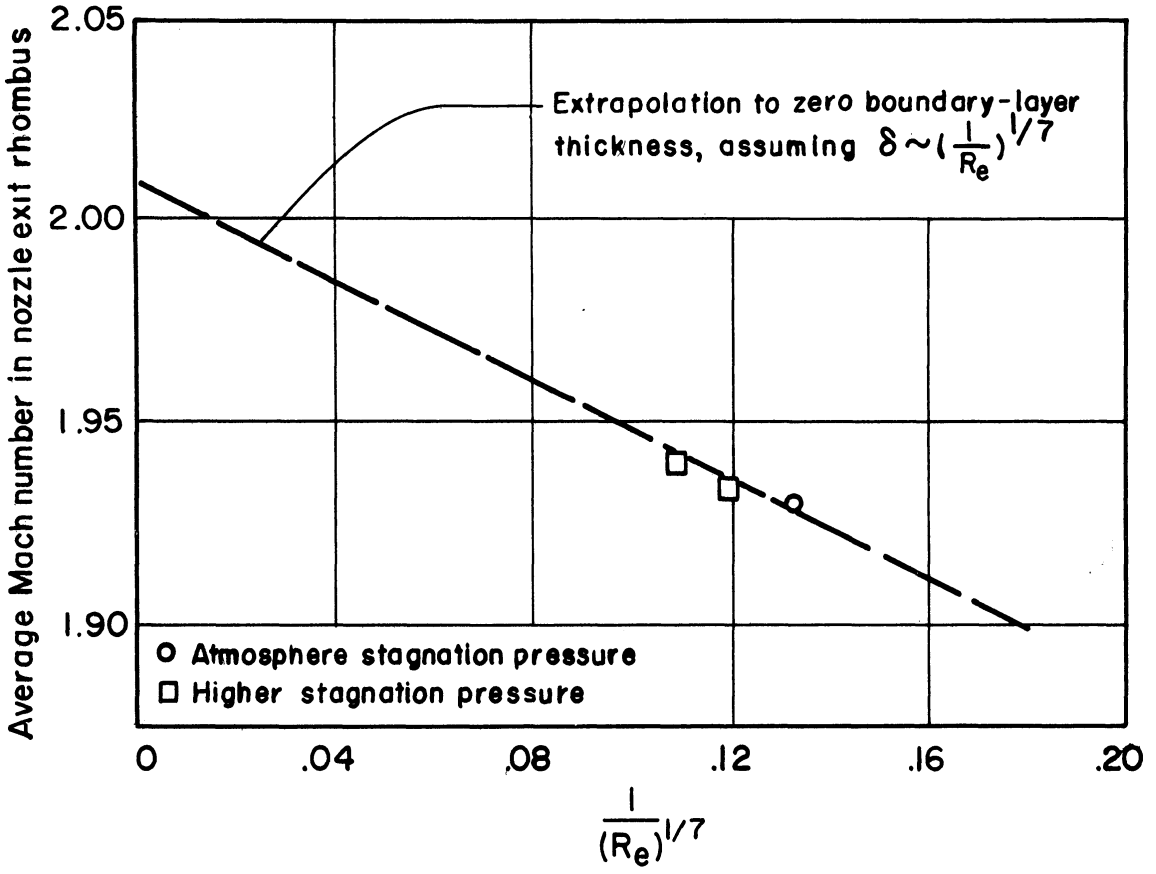

Fig. 19 Effect of Reynolds' Number on Average Test-Rhombus Mach Number

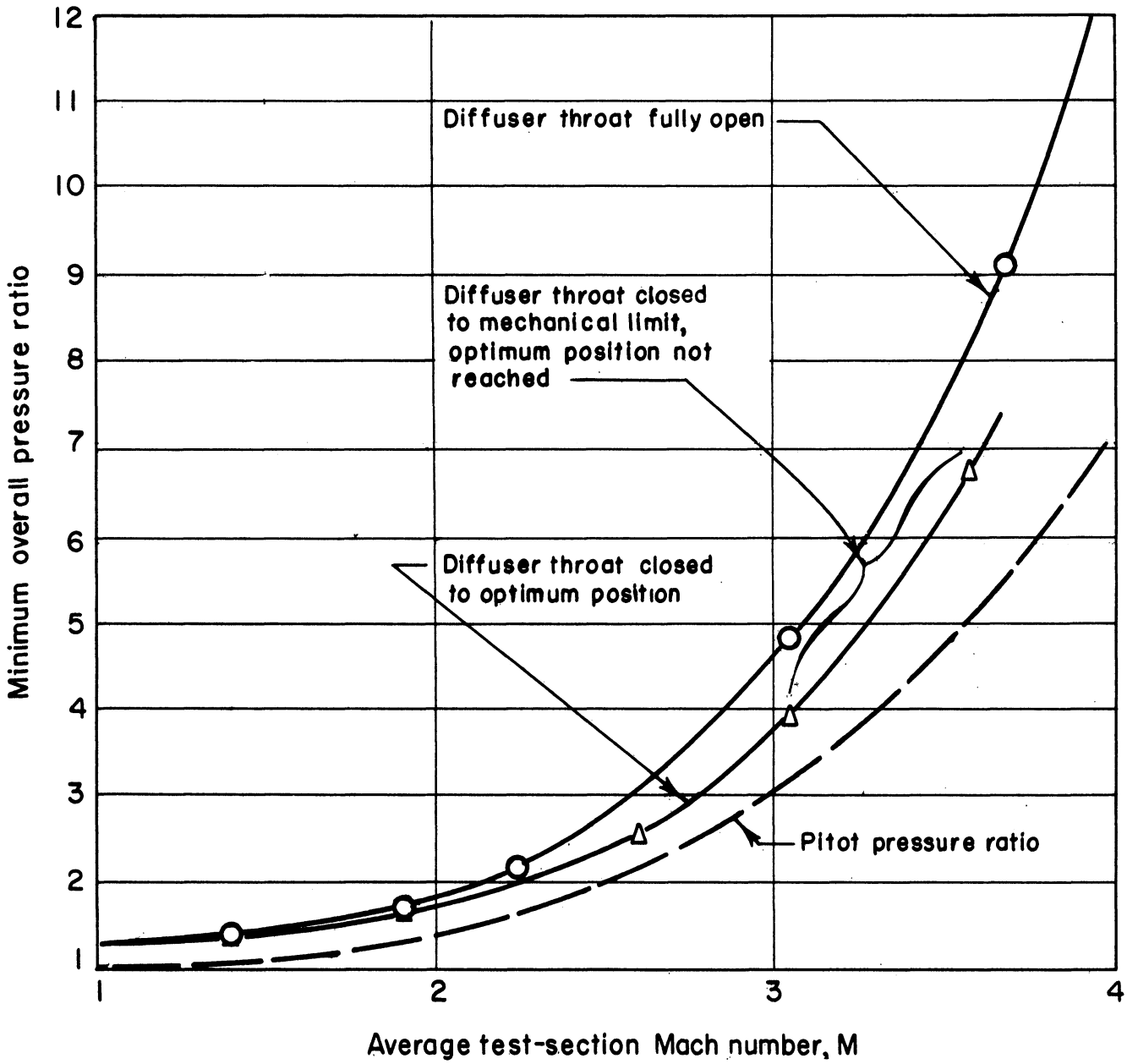

Fig. 20 Minimum Overall-Pressure Ratios for Two Diffuser Conditions. Nozzle with Theoretical Inviscid Contours

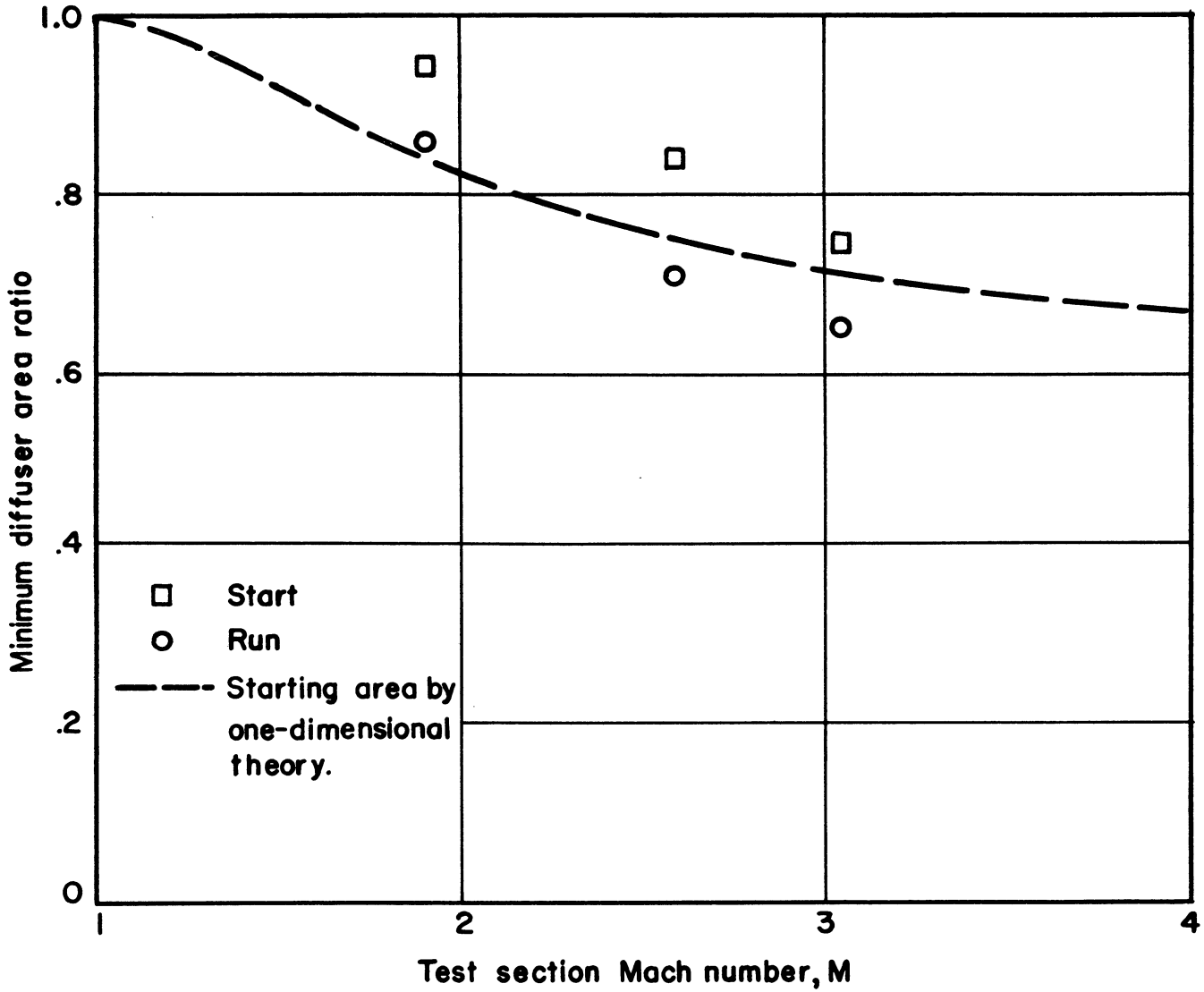

Fig. 21 Approximate Minimum Diffuser Area Ratios for Starting and for Running. 4- by 4-Inch Asymmetric Adjustable Nozzle with Original Contours. Tunnel Empty